The Morphological Characteristics of Choriocapillaris In the Fellow Eyes of Polypoidal Choroidal Vasculopathy.Co-authors

Huajui Wu
Fukushima Medical University
Yukinori Sugano
Fukushima Medical University
Kanako Itagaki
Fukushima Medical University
Akihito Kasai
Fukushima Medical University
Hiroaki Shintake
Fukushima Medical University
Tetsuju Sekiryu (sekiryu@fmu.ac.jp)
Fukushima Medical University

Research Article

Keywords: flow void (FV), polypoidal choroidal vasculopathy (PCV), indocyanine green angiography images, choroidal vascular hyperpermeability (CVH)

Posted Date: May 20th, 2021

DOI: https://doi.org/10.21203/rs.3.rs-537948/v1

Abstract

To evaluate the morphological characteristics of the flow void (FV) in the fellow eyes of the unilateral polypoidal choroidal vasculopathy (PCV).

52 eyes of PCV fellow eyes (PCVF) and 57 age-matched normal controls were recruited in this prospective study. The number of FV was analyzed according to the size which from 6×6-mm swept source optical coherence tomography angiography scans. We used indocyanine green angiography images to determine whether choroidal vascular hyperpermeability (CVH) has occurred. For the PCVF, the incidence of CVH was 70% (35 of 50. Two of participants were allergic to the dye.) The number of FV significantly lower in all sizes (P = .002), 400 ~ 500μm^2 (P = .002), 525 ~ 625μm^2 (P = .002) and 650 ~ 750μm^2 (P = .005). And the distribution significantly different in all sizes (P = .002), 400 ~ 500μm^2 (P = .001), 525 ~ 625μm^2 (P = .002) and 650 ~ 750μm^2 (P = .001) compared to the controls. And showed no differences in the size from 775 to 1125μm^2 between two groups. The area under the receiver operating characteristic curve of PCVF with CVH and controls was 0.93 (95% CI: 0.88 ~ 0.98) (P < .001). We found that the FV is a useful predictor for distinguishing the fellow eyes of PCV from normal eyes.

Introduction

Polypoidal choroidal vasculopathy (PCV) is a distinctive clinical entity causing choroidal neovascularization (CNV) in elderly persons proposed by Yannuzzi in 1990. It is usually diagnosed by f indocyanine green angiography (ICGA) examination to detect the polypoidal lesions or by indirect ophthalmoscopy to find the orange polypoidal structures. [1,2] The genetic predisposition may affect the pathophysiology of the PCV.[3] The fellow eyes of the PCV may be exposed to the background factors. And the PCV unaffected fellow eyes sometimes show pachychoroid features, despite unilateral cases. These facts suggested that pathognomonic changes may already begin in the fellow eyes of PCV. The analysis of the PCV fellow eyes may provide a clue to elucidate the pathogenesis of PCV.

The choroidal vasculature of PCV shows distinctive changes such as enlargement of vessels in Harllar's layer and attenuation of the small vessels in Sattler's layer. The changes of the choriocapillaris (CC) in the PCV would be expected. However, previous researchers [4] pointed out that there was no difference in vascular parameters of the choroidal vasculature including the CC between the pachychoroid eyes without disease and normal eyes in the study using optical coherence tomography angiography (OCTA). Other researchers [5] found that the CC flow deficit of PCV fellow eyes decreased, but did not reach the statistical difference compared to the age-matched control group. Since CC cannot be delineated directly with the current OCTA devices, careful consideration is required to reach a conclusion.

Swept-source optical coherence tomography angiography (SS-OCTA) is often used to evaluate the CC 2D images, due to the high scanning speed for evaluation. Although it has a wide depth range, the lateral resolution is lower than spectral-domain OCTA in general. For example, the lateral resolution of Plex Elite 9000 SS-OCTA (Carl Zeiss Meditec Inc, Dublin, California, USA), which was used in this research, was 20 μm.[6]

The diameter of the normal CC (16–20 μm) is smaller than the instrument resolution. [7–9] We could not see the CC structures directly on the SS-OCTA image. We used flow void (FV) of CC as a substitution of the CC structure, which was defined as the part of the CC slab without blood flow signals which diameter was bigger than the resolution of the SS-OCTA instrument.

Blood flow congestion in the choroid was postulated in PCV. We assumed two possible changes caused by congestion. One is that enlargement of capillary diameter due to congestion resulting FV decrease. Another is that ischemia due to congestion causing capillary dropout and FV increased. We speculated that the FV decreasing due to congestion may appear in the small size of FV in early stage. Then it may increase in size later. To clarify this issue, we need to analyze FV sorted by size. To our knowledge, the FV analysis by sizes in the eyes with PCV and the fellow eyes has not been reported.

In this study, we measured the number of FV in the groups stratified by the FV sizes to clarify the changes of FV in the fellow eyes of unilateral PCV.

Methods

Patients

This research was conducted following the Declaration of Helsinki.

This retrospective study was approved by the Institutional Review Board of Fukushima Medical University (No. 2020-091) and waived the individual consent for this analysis.

In this retrospective comparative study, we reviewed the medical records of 862 Japanese patients diagnosed with unilateral PCV between June 2017 and August 2020 at Fukushima Medical University Hospital, Fukushima, Japan.

The inclusion criterium was diagnosed with unilateral PCV, which evaluated by three ophthalmologists (T.S., Y.S., and A.K.) based on the presence of branching vascular networks, polypoidal lesions, and dilatated aneurysmal lesions on ICGA (TRC 50DX, Topcon, Tokyo, Japan) according to the published criteria.[1,2] Two of the participants were allergic to the ICGA dye, so we used indirect ophthalmoscopy to detect orange polypoidal structures for diagnosis. Fifty-seven fellow eyes of the patients diagnosed with unilateral retinal vein occlusion were selected as an age-matched normal control group. All RVO patients received FA for clinical evaluation and were confirmed no abnormality on FA in the contralateral eyes of RVO. All participants in both groups had no evidence of any retinal pathological change in the enrolled eyes.

The exclusion criteria for all eyes were as follows: 1. The eyes with any combined retinal diseases or intraocular diseases, such as macula hole, central serous chorioretinopathy, uveitis, and glaucoma. 2. The patients with any systemic diseases that affect CC circulation: uncontrolled hypertension, diabetes, gout, and neoplasm. 3. The refractive error is greater than -6 diopters. 4. Any observed drusen, RPE abnormality, or segmentation errors on the B-scan of SS-OCT images.

In which 771 patients met the exclusion criteria 1- 3 has been excluded. Then we reviewed the rest 91 patients' SS-OCT images. Among them, 39 patients met the exclusion criterium 4 and has been excluded.

All the patients who did not meet the exclusion criteria has been enrolled: 52 fellow eyes of 52 patients were PCV fellow eyes group (PCVF). According to the results of the choroidal vascular hyperpermeability (CVH) status, the PCVF was divided into two groups: PCV fellow eyes with CVH (CVH[+]) and PCV fellow eyes without CVH (CVH[-]). And 57 Japanese patients diagnosed with unilateral retinal vein occlusion (RVO) as controls.

Clinical examination

All included patients received comprehensive ophthalmic examinations, including indirect ophthalmoscopy, slit-lamp biomicroscopy, color, and red-free fundus photography, SS-OCTA, and ICGA at the first visit. RVO patients did not receive the ICGA for ethical reasons.

The choroidal vascular hyperpermeability (CVH) was defined as hyper fluorescence seen in the mid-phase (10 minutes after dye injected) of the ICGA images, the correspondent area of the OCTA images. (Fig. 1)

The CVH was evaluated by two masked ophthalmologists (H.W. and A.K.). The 5-minute images were as the reference and scored the ICGA images around 10-minute. The scores were defined as follows: All participants of the control group were scored 0. Scored 1 (PCV-): There was no distinguishable CVH in the area. Scored 2 (PCV[+]): There was obvious and strong CVH in the area. If the results were inconsistent, another experienced ophthalmologist (T.S.) will make the judgment.

The subfoveal choroidal thickness (SFCT) was measured by masked ophthalmologists (K.I. and H.S.) as the vertical distance between the RPE and the choroidoscleral border at the center of the fovea on the B-scan of SS-OCT through ImageJ software, version 1.52p (National Institutes of Health, Bethesda, Maryland, USA. https://imagej.nih.gov/ij/index.html).

Imaging processing

To analyze the FV, we conducted the binarization of the CC slab and grouped the FV according to our previous research.[10] (Fig. 2)

Briefly, we imported the CC slab bounded from 31 to 40μm beneath the RPE reference[11] and the correspondent en-face structural image to MATLAB R2019a. The compensation algorithm was used to eliminate the influence of the shadowing effect on the angiography images.[12] Then we imported the compensated images into ImageJ and processed the "Phansalkar local threshold" (radius= 5) for binarization.[13] After binarization, we processed "Analyze Particles" and "watershed irregular" [14] to remove the noise.

Since the center of the macula of some subjects was displacement from the center of the image (-210~ +455 μm), we performed manual correction to ensure that all images contain the same 5×5mm^2 area centered at the fovea. We applied "Analyze Particles" to summarize the FV in each interval.

Statistical analysis

Statistical calculations were performed by IBM SPSS V.26 for Windows (IBM Co., Armonk, New York, USA). The P-value lower than 0.05 was defined as the statistical significance. The Kolmogorov-Smirnov test was performed to detect the normality of distribution. Because the K-S test of FV number showed significance in most intervals, all variables were reported as median and quartile deviation. The independent samples median test adjusted by the Bonferroni correction has calculated the differences between groups. The independent samples Mann-Whitney U test was conducted to investigate the distribution differences. The Spearman's rank correlation coefficient was performed to evaluate the correlation between the FV and the CVH. The Youden index was used to determine the best cut-off point for the receiver operating characteristic (ROC) curve between the CVH[+] and the controls.

The size of flow void analysis

We compared the number and the distribution of the FV between PCVF and controls in the followed intervals to confirm the difference between the fellow eyes of PCV and normal eyes.

The primary outcome was the number of the flow void in different intervals among PCVF and controls.

We calculated the total area of FV sizes from 400μm^2 to 25000μm^2 for comparison (FVarea).

The number of the FV was divided into 7 groups.

FVall: The FV sizes from 400μm^2 to 25000μm^2 (from 16pixels to 1000pixels). FV500: The FV sizes from 400μm^2 to 500μm^2 (from 16pixels to 20pixels). FV625: The FV sizes from 525μm^2 to 625μm^2 (from 21pixels to 25pixels). FV750: The FV sizes from 650μm^2 to 750μm^2 (from 26pixels to 30pixels). FV875: The FV sizes from 775μm^2 to 875μm^2 (from 31pixels to 35pixels). FV1000: The FV sizes from 900μm^2 to 1000μm^2 (from 36pixels to 40pixels). FV1125: The FV sizes from 1025μm^2 to 1125μm^2 (from 41pixels to 45pixels).

The relationship between choroidal vascular hyperpermeability and the flow void

To investigate the relationship between FV and CVH status, we performed Spearman's rank correlation analysis among the FV and CVH status in all intervals.

Then we compared the number of FV between CVH[+], CVH[-] and controls in each interval to confirm the influence of CVH.

Receiver operating characteristic curve analysis

We used binary logistic regression analysis for CVH[+] and controls depending on the results of FV and CVH analysis.

The FV smaller than 750μm^2 were grouped every 25μm^2 (1 pixel) and subjected to binary logistic regression analysis after standardization.

We performed the receiver operating characteristic curve analysis to find a cut-off value for maximizing sensitivity and specificity to discriminate two groups.

Results

Baseline characteristics

The mean age was 68.6 ± 7.8 (51- 84 years) in the PCV fellow eyes and 67.9 ± 8.7 (47- 84 years) in age-matched controls. There was no difference between the two groups in age (P=.677), refractive error (P=.524), and subfoveal choroidal thickness (P=.126).

The incidence of CVH was 70% in PCVF (35 of 50 participants. Two of the participants were allergic to the ICGA dye and were excluded from the CVH analysis.)

The demographic characteristics of the groups are shown in Table 1.

Validation of the normal distribution

The Kolmogorov-Smirnov test results among two groups was: age: P= .200, refractive error: P= .200, SFCT: P= .051, FVall: P= .042, FV500: P< .001, FV625: P= .001, FV750: P= .086, FV875: P= .200, FV1000: P= .200, FV1125: P= .060, FVarea: P=.014.

The number of the flow void

The relation between the FV size and the FV number is presented in Fig3.

There were no differences in FVarea among the two groups: Median test (P=.920), Mann-Whitney U test (P=.125).

In the comparison of PCVF and the controls, the number of FV of PCVF in all intervals were lower than controls. (Fig.3) (Table 2.) There was statistical significance compared to the controls in following intervals: FVall (P< .001), FV500 (P< .001), FV625 (P= .002) and FV750 (P= .002). And showed no difference in FV875 (P= .934), FV1000 (P= .920) and FV1125 (P= .948). (Fig.3, P1)

The distribution among two groups showed significant different, and the PCVF group showed higher central tendency in following intervals: FVall (P< .001), FV500 (P< .001), FV625 (P= .002) and FV750 (P= .002). And showed no difference in FV875 (P= .134), FV1000 (P= .429) and FV1125 (P= .927). (Fig.3, P2)

The analysis among the FV and CVH

In the comparation among 107 participants, the number of the FV in the following intervals were significantly negative correlated with the CVH status: FVall (r= -.36, P< .001), FV500 (r= -.44, P< .001), FV625 (r= -.31, P= .001) and FV750 (r= -.31, P= .001). (Table 3.)

In the comparison of CVH[+], CVH[-] and controls, the number of FV significant lower in the CVH[+] compared to the controls in following intervals: FVall (P< .001), FV500 (P< .001), FV625 (P= .001) and FV750 (P= .016). Showed no difference in FV875 (P= .223), FV1000 (P= .516) and FV1125 (P= .538). There were no differences among CVH[+] and CVH[-], and among CVH[-] and controls in all intervals (all P> .05). (Table 4.)

The receiver operating characteristic curve of CVH[+] and controls.

Based on the Youden index, the cut-off points of FV for predicting the fellow eyes of PCV with CVH was 0.51, with a sensitivity= 91.4%, specificity = 86.0%, the area under the curve (AUC) was 0.93 (95% CI: 0.88~ 0.98) (P< .001). (Fig.4)

Discussion

In this retrospective research, the number of FV size smaller than 750μm^2 substantially decreased in the fellow eyes of PCV compared to the controls whereas the total FV area was not different between the two groups. Most of the PCV fellow eyes showed CVH (70%, 35 of 50). The severity of CVH was negatively correlated to the number of FV.

This is the first study that found the difference between the fellow eyes of PCV and normal controls by using a non-invasive, commercially available SS-OCTA instrument.

Previous studies of ICGA had shown that the pathological changes of PCV and central serous chorioretinopathy had similar choroidal vascular circulatory disturbance.[15] For the very early stage of the PCV which the choroid shows no pathological changes, recent researches[4,5,16] cannot tell the difference. However, we found that the FV decreased in the fellow eyes of PCV compared to the controls.

There were different studies on the protocol of CC slab obtained by OCTA.[11,17–20] We chose the protocol that has been used more in other studies as the standard of this research.[11] And used our published FV analysis method: Grouped the FV by size and performed statistical analysis on each group.[10] Because of the power-law distribution: The small sizes had relatively large numbers.[21] (Fig. 5) Once the pathological change occurred on the small FV, it may not be big enough to affect the average size; once the pathological change

occurred on the big FV, which was too scarce to affect the total number and size of FV. Grouping analysis strategy can avoid these problems and effectively detect the difference of FV in the specific interval that did not appear in previous studies. Evaluating the number of small sizes of FV has another advantage. Pachydrusen is relatively large size drusen frequently appearing in PCV[22]. Drusen area can decrease the penetration of OCTA laser to underestimating the FV density[19]. Our grouping strategy can decrease the influence of pachydrusen on calculating the FV numbers rather than the area.

The upper limit of the interval was 1125 μm^2. Due to the power-law distribution[23], the FV larger than 1125 μm^2 contained less than 5% of the total, which were excluded from the statistics. The FV smaller than 750μm^2 was decreased because the small FV was more sensitive to the radius changes (e.g. Two FV which the original areas were 20μm^2 and 1125μm^2, when the radius was reduced by 1μm, the area reduced 40% and 6%.) Therefore, the FV of all sizes will be affected when hyperpermeability occurred, and the FV with a small size can be more substantially affected. The decreasing of the FV represented the increase of the blood flow signal area, which might because of the hyperpermeability of CC, the increase of vessel diameter, or the increase of the blood flow.

Based on the Youden index, our model has high sensitivity (91.4%) and specificity (86.0%). Therefore, this model with the number of FV as a predictor is helpful (AUC = .93). This finding can give a clue for the early screening of PCV in the future.

Recently, OCTA can effectively detect the typical pathological manifestations of PCV.[24] A recent study had similar results to ours, that the proportion of the choriocapillaris flow deficit area of PCV fellow eyes has a decreasing trend, but there was no statistical difference compared with the age-matched control group[5]. However, in our research, the number of FV in small sizes decreased compared to controls, and the total area has no difference.

We believe that the insignificant difference in FV of their research was due to the proportion area analysis strategy, or the impact of underlying diseases, which resulted in an overall decrease trend but not statistically significant. Many systemic and ocular factors could change the choroidal circulation, that is age[25–27], choroidal thickness[28], intraocular pressure[29,30], and systemic diseases[31–36]. These factors may also change the morphology of the CC resulting in the FV changes. Previous research revealed that the size of FV in diabetic retinopathy eyes was larger than the normal elderly eyes, and this trend was positively correlated with the severity of diabetic retinopathy.[31–33] Hypertension can also increase the size and the number of FV.[34–36] The eyes with advanced Age-Related Eye Disease Study Category stage will cause the increase in size and number of the FV.[37,38] We excluded the subjects who had suspected drusen or RPE abnormality on the B-scan and the diseases that had impacts on the CC structure. It can be considered that the difference in the FV was not from age or other systematic diseases.

Previous histopathology studies pointed out that the CC of the eyes with advanced PCV can have plumped endothelial cells, primitive or narrow lumen, or dilated vessels.[39–41] Our result showed that the reduction of the CVH status was negatively correlated with the number of the FV. However, the number of the FV of CVH[-] was between the CVH[+] and the control group and showed no significant difference (Table. 4), we think there

are two possibilities: 1. CVH[-] is in the earlier stage of PCV than CVH[+], the severity of the CVH does not reach an observable level. 2. Although most of the fellow eyes of PCV tended to evolve into PCV in the future, not all of them. The CVH[-] are normal eyes at the beginning and will not evolve into PCV.

CVH was more commonly seen in the eyes with pachychoroid[42], but it also occurred in the PCV and fellow eyes.[43–48] A previous study in monkeys and rabbits had proved that the dye of ICGA was exuded and the CVH was formed due to vascular endothelial damage,[49] suggested that CVH[+] exhibits vessel abnormalities at the innermost choroid. Based on the mechanism of OCTA, the blood flow signals came from the movement of red blood cells[6], the decrease of the area without blood flow signals (FV) means that the area occupied by red blood cells increased, however, the red blood cells should not exist outside the vessels. In other words, at least the diameter of the CC parallel to the RPE increased.

One possibility is that the diameters perpendicular to the RPE and parallel to the RPE were both dilated, induce the CC endothelial damage, which causes the leakage of ICGA dye and showed hyperpermeability of CC. At the same time, due to endothelial damage, the concentration of vascular endothelial growth factors increased. Which in turn further promotes vasodilation and eventually forms pachychoroid disease. Another possibility is that due to the vasodilation of the choroidal vessels, the CC was squeezed toward the RPE, causing mechanical deformation of the CC (the diameter of the CC perpendicular to the RPE decreased and the diameter parallel to the RPE increased, like a squashed straw). As the CC lumen is squeezed, local blood flow can be slowed down and occurred turbulence. Slow blood flow and turbulence cause thrombosis and may be further related to the pathogenesis of PCV. These two assumptions have the same characteristics on the CC slab of SS-OCTA: The diameter parallel to the slab of CC increased, and the FV became smaller. Our result shows that the hyperpermeability of PCVF occurs earlier than the detectable RPE abnormality on the B-scan of SS-OCT.

The Mann-Whitney U test shows similar results (Fig. 3): Compared with the control group, the distribution of PCVF has a higher central tendency. As the size of the FV became smaller, these small FVs will fall into the previous interval during analysis, makes the minimum values disappear and the maximum values closer to the median. Once the FV size is smaller than 400μm^2, which cannot be detected and will be discarded. So, the overall number is reduced, and the distribution has a higher central tendency.

The limitations are retrospective nature and small sample size. We strictly controlled the underlying conditions, which limited the generalizability of our findings in clinical practice. We used the watershed method to separate the large FV, which may lead to underestimation of the large FV and overestimation of the small FV in quantity. Besides, CVH can also occur in other diseases, including central serous chorioretinopathy. It needs further research to specifically distinguish the CVH of PCV from other causes in the future.

In conclusion, most of the PCV fellow eyes in this research occurred choroidal vascular hyperpermeability, which CVH should be the earliest sign of PCV when other inspections were normal. The FV is an effective biomarker to discriminates the early stage of PCV from normal eyes.

Declarations

Competing interests

The authors declare no competing interests.

Data Availability

The datasets generated and analyzed during the current study are available from the corresponding author on reasonable request.

Author contributions

H.W. and T.S. designed the study.

T.S. wrote the application to the ethics committee.

T.S., Y.S., and A.K. performed the ophthalmological examinations.

H.W., K.I., and H.S. reviewed the medical records and OCTA images and collected all imaging data.

H.W., A.K., and T.S. evaluated CVH status.

K.I. and H.S. evaluated SFCT in all images.

H.W. and Y.S. performed statistical analyses.

All authors wrote and reviewed the final version of the manuscript.

References

1. Yannuzzi, L. A., Sorenson, J., Spaide, R. F. & Lipson, B. Idiopathic polypoidal choroidal vasculopathy (IPCV). *Retina.* **10**, 1–8 (1990).
2. Spaide, R. F., Yannuzzi, L. A., Slakter, J. S., Sorenson, J. & Orlach, D. A. Indocyanine green videoangiography of idiopathic polypoidal choroidal vasculopathy. *Retina.* **15**, 100–110 (1995).
3. Sho, K. *et al.* Polypoidal choroidal vasculopathy: incidence, demographic features, and clinical characteristics. *Arch Ophthalmol.* **121**, 1392–1396 (2003).
4. Spaide, R. F. & Ledesma-Gil, G. Choriocapillaris Vascular Parameters in Normal Eyes and Those with Pachychoroid with and without Disease.*Retina*(2020).
5. Luo, M. *et al.* Comparison of choriocapillary flow density between fellow eyes of polypoidal choroidal vasculopathy and neovascular age-related macular degeneration. *BMC Ophthalmol.* **20**, 162 (2020).
6. Kashani, A. H. *et al.* Optical coherence tomography angiography: A comprehensive review of current methods and clinical applications. *Prog Retin Eye Res.* **60**, 66–100 (2017).
7. Olver, J. M. Functional anatomy of the choroidal circulation: methyl methacrylate casting of human choroid. *Eye (Lond).* **4** (Pt 2), 262–272 (1990).
8. Yoneya, S. & Tso, M. O. Angioarchitecture of the human choroid. *Arch Ophthalmol.* **105**, 681–687 (1987).

9. Fryczkowski, A. W. Anatomical and functional choroidal lobuli. *Int Ophthalmol.* **18**, 131–141 (1994).
10. Huajui Wu *et al.* A modified measuring method to investigate the choriocapillaris flow void of polypoidal choroidal vasculopathy with swept source optical coherence tomography angiography. *Quant Imaging Med Surg.* **11** (7), 3146–3156 (2021).
11. Spaide, R. F., Fujimoto, J. G. & Waheed, N. K. Image artifacts in Optical coherence tomography angiography. *Retina.* **35**, 2163–2180 (2015).
12. Zhang, A., Zhang, Q. & Wang, R. K. Minimizing projection artifacts for accurate presentation of choroidal neovascularization in OCT micro-angiography. *Biomed Opt Express.* **6**, 4130–4143 (2015).
13. Neerad, P., Sumit, M., Ashish, S. & Madhuri, J. Adaptive local thresholding for detection of nuclei in diversity stained cytology images. in 2011 *International Conference on Communications and Signal Processing* 218–220 (2011).
14. Soille, P. & Vincent, L. Determining watersheds in digital pictures via flooding simulations(SPIE, 1990).
15. Guyer, D. R. *et al.* Digital indocyanine-green videoangiography of occult choroidal neovascularization. *Ophthalmology.* **101**, 1727–1735 discussion 1735 – 1727 (1994).
16. Baek, J., Cheung, C. M. G., Jeon, S., Lee, J. H. & Lee, W. K. Polypoidal Choroidal Vasculopathy: Outer Retinal and Choroidal Changes and Neovascularization Development in the Fellow Eye. *Invest Ophthalmol Vis Sci.* **60**, 590–598 (2019).
17. Chu, Z., Gregori, G., Rosenfeld, P. J. & Wang, R. K. Quantification of Choriocapillaris with Optical Coherence Tomography Angiography: A Comparison Study. *Am J Ophthalmol.* **208**, 111–123 (2019).
18. Byon, I., Nassisi, M., Borrelli, E. & Sadda, S. R. Impact of Slab Selection on Quantification of Choriocapillaris Flow Deficits by Optical Coherence Tomography Angiography. *Am J Ophthalmol.* **208**, 397–405 (2019).
19. Chu, Z. *et al.* Quantification of Choriocapillaris with Phansalkar Local Thresholding: Pitfalls to Avoid. *Am J Ophthalmol.* **213**, 161–176 (2020).
20. Chu, Z., Zhang, Q., Gregori, G., Rosenfeld, P. J. & Wang, R. K. Guidelines for Imaging the Choriocapillaris Using OCT Angiography. *Am J Ophthalmol.* **222**, 92–101 (2020).
21. Newman, M. E. J. Power laws, Pareto distributions and Zipf's law. *Contemp. Phys.* **46**, 323–351 (2005).
22. Spaide, R. F., DISEASE EXPRESSION IN & NONEXUDATIVE AGE-RELATED MACULAR DEGENERATION VARIES WITH CHOROIDAL THICKNESS. *Retina.* **38**, 708–716 (2018).
23. Spaide, R. F. Choriocapillaris Flow Features Follow a Power Law Distribution: Implications for Characterization and Mechanisms of Disease Progression. *Am J Ophthalmol.* **170**, 58–67 (2016).
24. Kim, K. *et al.* A Comparison Study of Polypoidal Choroidal Vasculopathy Imaged with Indocyanine Green Angiography and Swept Source OCT Angiography.*Am J Ophthalmol*(2020).
25. Yun, C., Nam, K. T., Park, S., Hwang, S. Y. & Oh, J. Features of the choriocapillaris on four different optical coherence tomography angiography devices. *Int Ophthalmol.* **40**, 325–333 (2020).
26. Zheng, F. *et al.* Age-dependent Changes in the Macular Choriocapillaris of Normal Eyes Imaged With Swept-Source Optical Coherence Tomography Angiography. *Am J Ophthalmol.* **200**, 110–122 (2019).

27. Sacconi, R. *et al.* Quantitative changes in the ageing choriocapillaris as measured by swept source optical coherence tomography angiography. *Br J Ophthalmol.* **103**, 1320–1326 (2019).
28. Rochepeau, C. *et al.* Optical Coherence Tomography Angiography Quantitative Assessment of Choriocapillaris Blood Flow in Central Serous Chorioretinopathy. *Am J Ophthalmol.* **194**, 26–34 (2018).
29. Mammo, Z. *et al.* Quantitative Optical Coherence Tomography Angiography of Radial Peripapillary Capillaries in Glaucoma, Glaucoma Suspect, and Normal Eyes. *Am J Ophthalmol.* **170**, 41–49 (2016).
30. Yarmohammadi, A. *et al.* Optical Coherence Tomography Angiography Vessel Density in Healthy, Glaucoma Suspect, and Glaucoma Eyes. *Invest Ophthalmol Vis Sci.* **57**, Oct451–459 (2016).
31. Thompson, I. A., Durrani, A. K. & Patel, S. Optical coherence tomography angiography characteristics in diabetic patients without clinical diabetic retinopathy. *Eye (Lond).* **33**, 648–652 (2019).
32. Cao, D. *et al.* Optical coherence tomography angiography discerns preclinical diabetic retinopathy in eyes of patients with type 2 diabetes without clinical diabetic retinopathy. *Acta Diabetol.* **55**, 469–477 (2018).
33. Dodo, Y. *et al.* Clinical relevance of reduced decorrelation signals in the diabetic inner choroid on optical coherence tomography angiography. *Sci Rep.* **7**, 5227 (2017).
34. Bosch, A. J. *et al.* Retinal capillary rarefaction in patients with untreated mild-moderate hypertension. *BMC Cardiovasc Disord.* **17**, 300 (2017).
35. Jumar, A. *et al.* Improvement in Retinal Capillary Rarefaction After Valsartan Treatment in Hypertensive Patients. *J Clin Hypertens (Greenwich).* **18**, 1112–1118 (2016).
36. Sun, C. *et al.* Systemic hypertension associated retinal microvascular changes can be detected with optical coherence tomography angiography. *Sci Rep.* **10**, 9580 (2020).
37. Mullins, R. F., Johnson, M. N., Faidley, E. A., Skeie, J. M. & Huang, J. Choriocapillaris vascular dropout related to density of drusen in human eyes with early age-related macular degeneration. *Invest Ophthalmol Vis Sci.* **52**, 1606–1612 (2011).
38. Biesemeier, A., Taubitz, T., Julien, S., Yoeruek, E. & Schraermeyer, U. Choriocapillaris breakdown precedes retinal degeneration in age-related macular degeneration. *Neurobiol Aging.* **35**, 2562–2573 (2014).
39. Okubo, A., Sameshima, M., Uemura, A., Kanda, S. & Ohba, N. Clinicopathological correlation of polypoidal choroidal vasculopathy revealed by ultrastructural study. *Br J Ophthalmol.* **86**, 1093–1098 (2002).
40. Lafaut, B. A., Aisenbrey, S., Van den Broecke, C., Bartz-Schmidt, K. U. & Heimann, K. Polypoidal choroidal vasculopathy pattern in age-related macular degeneration: a clinicopathologic correlation. *Retina.* **20**, 650–654 (2000).
41. Moussa, K. *et al.* POLYPOIDAL CHOROIDAL VASCULOPATHY: A CLINICOPATHOLOGIC STUDY. *Retin Cases Brief Rep.* **11 Suppl** (1), S128–s131 (2017).
42. Borooah, S. *et al.* Pachychoroid spectrum disease.*Acta Ophthalmol*(2020).
43. Yanagi, Y. *et al.* CHOROIDAL VASCULAR HYPERPERMEABILITY AS A PREDICTOR OF TREATMENT RESPONSE FOR POLYPOIDAL CHOROIDAL VASCULOPATHY. *Retina.* **38**, 1509–1517 (2018).
44. Lee, J., Byeon, S. H., PREVALENCE AND CLINICAL CHARACTERISTICS & OF PACHYDRUSEN IN POLYPOIDAL CHOROIDAL VASCULOPATHY. Multimodal Image Study. *Retina.* **39**, 670–678 (2019).

45. Koizumi, H., Yamagishi, T., Yamazaki, T. & Kinoshita, S. Relationship between clinical characteristics of polypoidal choroidal vasculopathy and choroidal vascular hyperpermeability. Am J Ophthalmol 155, 305–313 e301(2013).
46. Chung, S. E., Kang, S. W., Kim, J. H., Kim, Y. T. & Park, D. Y. Engorgement of vortex vein and polypoidal choroidal vasculopathy. *Retina.* **33**, 834–840 (2013).
47. Ryu, G., Moon, C., van Hemert, J. & Sagong, M. Quantitative analysis of choroidal vasculature in polypoidal choroidal vasculopathy using ultra-widefield indocyanine green angiography. *Sci Rep.* **10**, 18272 (2020).
48. Sasahara, M. *et al.* Polypoidal choroidal vasculopathy with choroidal vascular hyperpermeability. *Am J Ophthalmol.* **142**, 601–607 (2006).
49. Yoshioka, H. [The etiology of central serous chorioretinopathy]. *Nippon Ganka Gakkai Zasshi.* **95**, 1181–1195 (1991).

Tables

Table 1
Characteristics of Participant Groups (Mean ± SD)

Groups	PCVF	Control	P-value†
No. of eyes (No. of right eyes)	52 (27)	57 (17)	.103
No. of Male	41 (78.8%)	22 (38.6%)	< .001**
Age (years)	68.6 ± 7.8	67.9 ± 8.7	.677
Re (Diopter)	0.5 ± 1.8	0.3 ± 1.7	.524
SFCT (μm)	241.2 ± 82.8	220.3 ± 53.9	.126

†Student t-test. **P < .01

Re: Refractive error, SFCT: Subfoveal Choroidal thickness.

PCVF: The fellow eyes of PCV. Control: The age-matched normal control group.

Table 2
The Number of The Flow Void in Different Sizes.

Intervals of FV sizes	Groups				P-value	
	Control (n = 57) (Median, QD)	PCVF (n = 52) (Median, QD)	95% CI		Median Test†	U Test‡
FVall (0 ~ 25000 μm^2)	9113.0 , 2025.5	8260.0 , 1294.0	6773.8~	11166.8	P < .001**	P < .001**
FV500 (400 ~ 500 μm^2)	4065.0 , 1484.5	2857.5 , 1067.0	2574.0~	4576.5	P < .001**	P < .001**
FV625 (525 ~ 625 μm^2)	1645.0 , 396.0	1461.0 , 264.3	1293.8~	1898.0	P = .002**	P = .002**
FV750 (650 ~ 750 μm^2)	1152.0 , 219.0	1050.0 , 149.3	885.5~	1352.8	P = .002**	P = .002**
FV875 (775 ~ 875 μm^2)	774.0 , 139.5	771.0 , 135.8	566.8~	969.3	P = .934	P = .134
FV1000 (900 ~ 1000 μm^2)	543.0 , 120.0	539.5 , 97.8	337.3~	673.3	P = .920	P = .429
FV1125 (1025 ~ 1125 μm^2)	373.0 , 83.5	372.5 , 96.5	209.8~	506.5	P = .948	P = .927
FVarea (μm^2)	6.1 ,1.1	6.2 ,1.2	4.6~	8.5	P = .920	P = .125

† Independent-Samples Median Test, ‡ Independent-Samples Mann-Whitney U Test. **P < .01

QD: Quartile deviation. Control: The age-matched normal control group. PCVF: The fellow eyes of PCV.

Table 3
The Correlation Between Choroid Vascular Hyperpermeability and Flow Void.

Intervals of FV sizes	r	P-value†
FVall (0 ~ 25000 μm^2)	− .36	P < .001**
FV500 (400 ~ 500 μm^2)	− .44	P < .001**
FV625 (525 ~ 625 μm^2)	− .32	P = .001**
FV750 (650 ~ 750 μm^2)	− .31	P = .001**
FV875 (775 ~ 875 μm^2)	− .17	P = .087
FV1000 (900 ~ 1000 μm^2)	− .08	P = .396
FV1125 (1025 ~ 1125 μm^2)	.01	P = .936

† Spearman's rank correlation coefficient. **P < .01

FV: The flow void of choriocapillaris.

Table 4
The Number of The Flow Void in Different CVH Status. †

Intervals of FV sizes	Control (n = 57) (Median, QD)		CVH[-] (n = 15) (Median, QD)		CVH[+] (n = 35) (Median, QD)		P-value Control vs. CVH[-]	P-value CVH[-] vs. CVH[+]	P-value Control vs. CVH[+]
FVall (0 ~ 25,000 μm^2)	9,113.0	, 2,025.5	8,525.0	, 1,968.0	8,240.0	, 1,043.0	P = 1.000	P = 1.000	P < .001**
FV500 (400 ~ 500 μm^2)	4,065.0	, 1,484.5	3,015.0	, 1,240.0	2,851.0	, 274.0	P = .127	P = 1.000	P < .001**
FV625 (525 ~ 625 μm^2)	1,645.0	, 396.0	1,518.0	, 265.0	1,442.0	, 153.0	P = .440	P = 1.000	P = .001**
FV750 (650 ~ 750 μm^2)	1,152.0	, 219.0	1,064.0	, 250.0	1,050.0	, 155.0	P = .440	P = 1.000	P = .016*
FV875 (775 ~ 875 μm^2)	774.0	, 139.5	793.0	, 97.0	769.0	, 116.0	P = .223	P = .223	P = .223
FV1000 (900 ~ 1,000 μm^2)	543.0	, 120.0	563.0	, 86.0	537.0	, 109.0	P = .516	P = .516	P = .516
FV1125 (1,025 ~ 1,125 μm^2)	373.0	, 83.5	391.0	, 60.0	369.0	, 110.0	P = .538	P = .538	P = .538

Intervals of FV sizes	Control (n = 57) (Median, QD)	CVH[-] (n = 15) (Median, QD)	CVH[+] (n = 35) (Median, QD)	P-value Control vs. CVH[-]	P-value CVH[-] vs. CVH[+]	P-value Control vs. CVH[+]

† Independent-Samples Median Test, adjusted by the Bonferroni correction. *P < .05, **P < .01

QD: Quartile deviation.

FV: The flow void of choriocapillaris. Control: The age-matched normal control group. CVH[-]: The fellow eyes of PCV without choroidal vascular hyperpermeability. CVH[+]: The fellow eyes of PCV with choroidal vascular hyperpermeability.

Figures

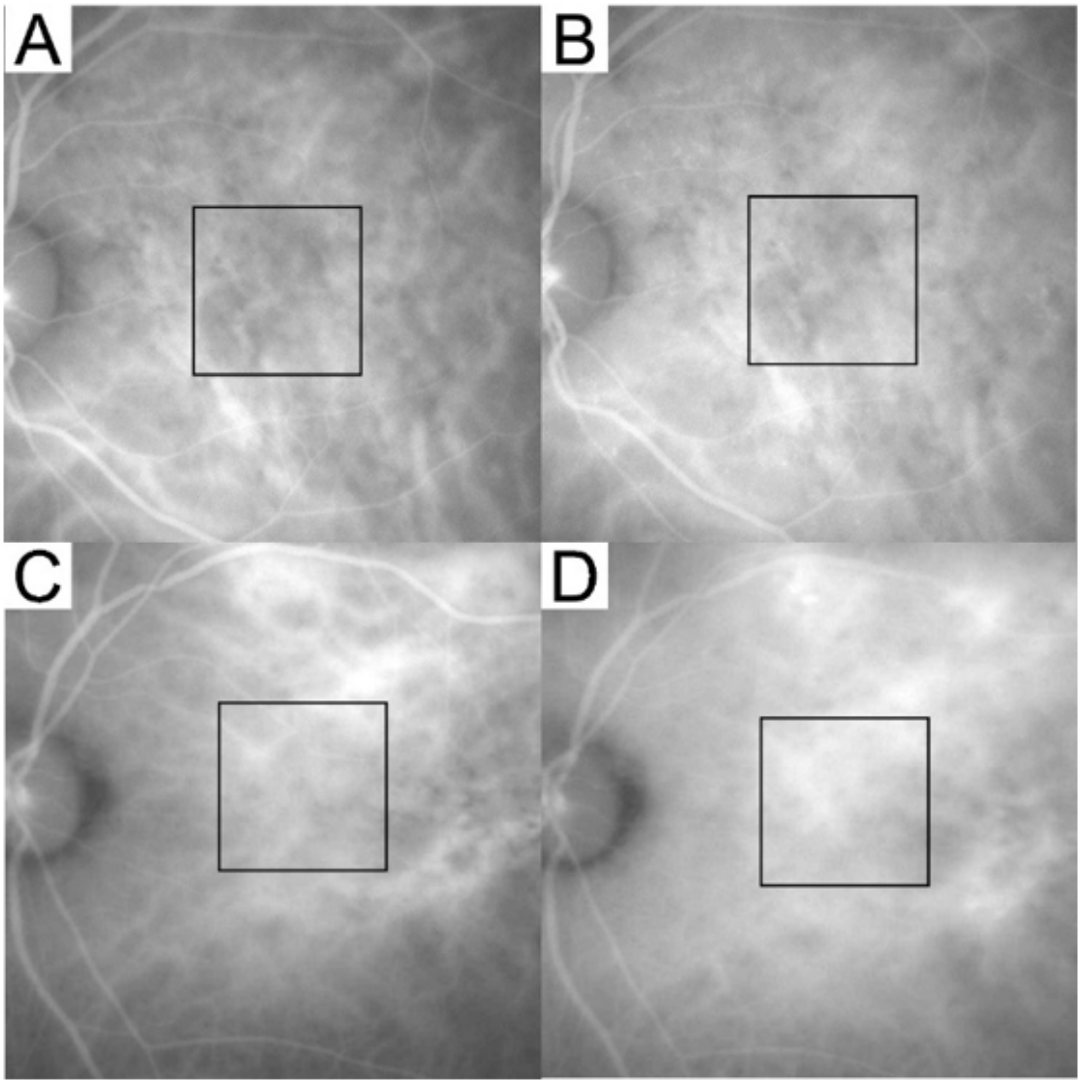

Figure 1

The demonstration of the choroidal vascular hyperpermeability severity grading. The square represents a 5×5-mm2 area corresponded to the OCTA image. (A and C) The left column is the ICGA images taken 5 minutes after the dye injection, as a benchmark for comparison. (B and D) The right column is the ICGA images taken about 10 minutes after the dye injection, to evaluate the CVH status in the square. (B) Scored 1 (CVH[-]): Compared with A, B has no choroidal vascular hyperpermeability. (D) Scored 2 (CVH[+]): Compared with C, D has obvious and strong choroidal vascular hyperpermeability. CVH[-]: The fellow eyes of PCV without choroidal vascular hyperpermeability. CVH[+]: The fellow eyes of PCV with choroidal vascular hyperpermeability.

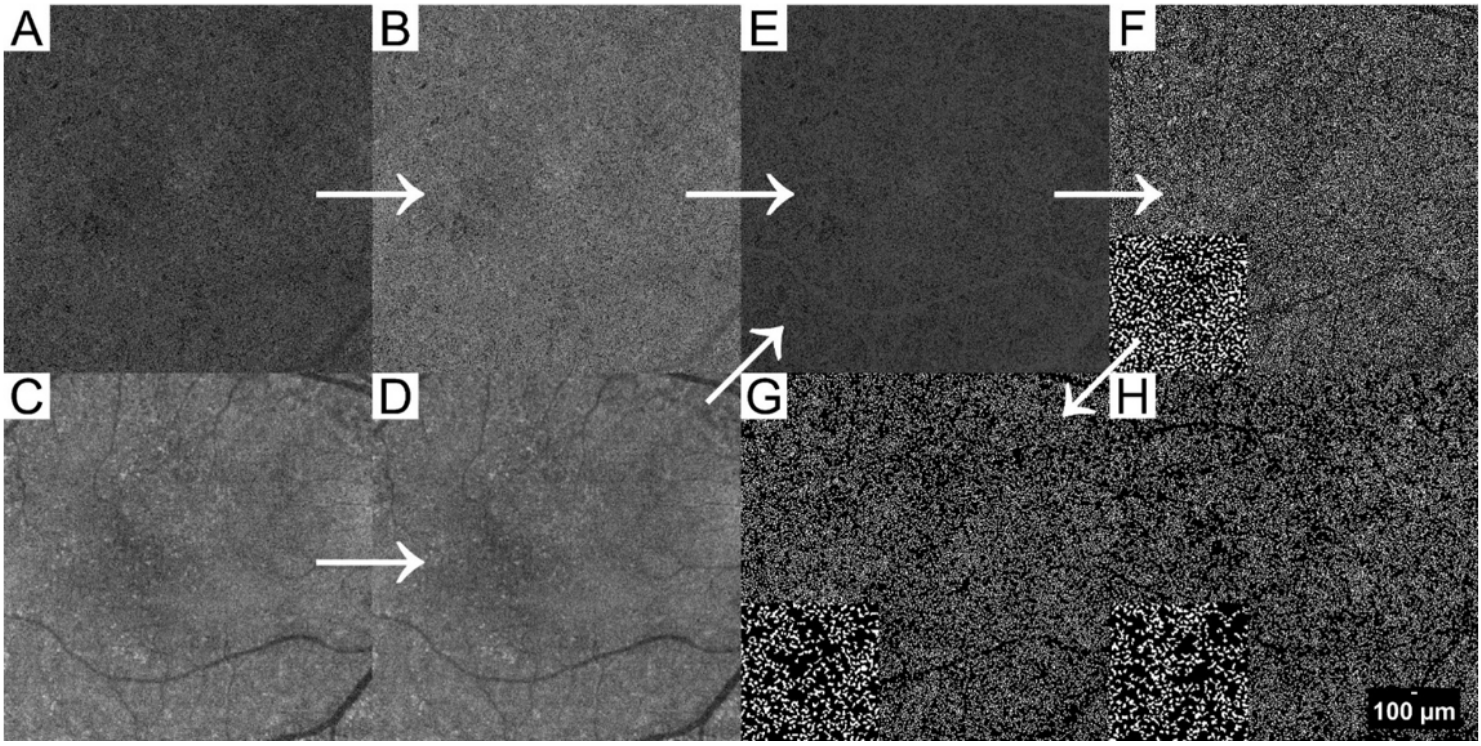

Figure 2

The demonstration of image processing protocol A 64 years old normal eye. The white arrows demonstrate our image process protocol. (A and C) The original angiography image and corresponded structural OCT image exported from the SS-OCT machine. (B and D) Images after Normalization and resize. (E) After enhancement, the shadow of superficial vessels has been eliminated. (F) A FV image after binarization. White parts represented the FV and noise. Composition: 1mm2 centered at the image. The FV was incorrectly connected into clusters because of noise. (G) The result after removing the noise. Composition: 1mm2 centered at the image. The FV was divided into reasonable sizes. (H) A 66 years old PCV fellow eye with CVH, showed sparse FV. Composition: 1mm2 centered at the image. FV: The flow void of choriocapillaris. CVH: Choroidal vascular hyperpermeability.

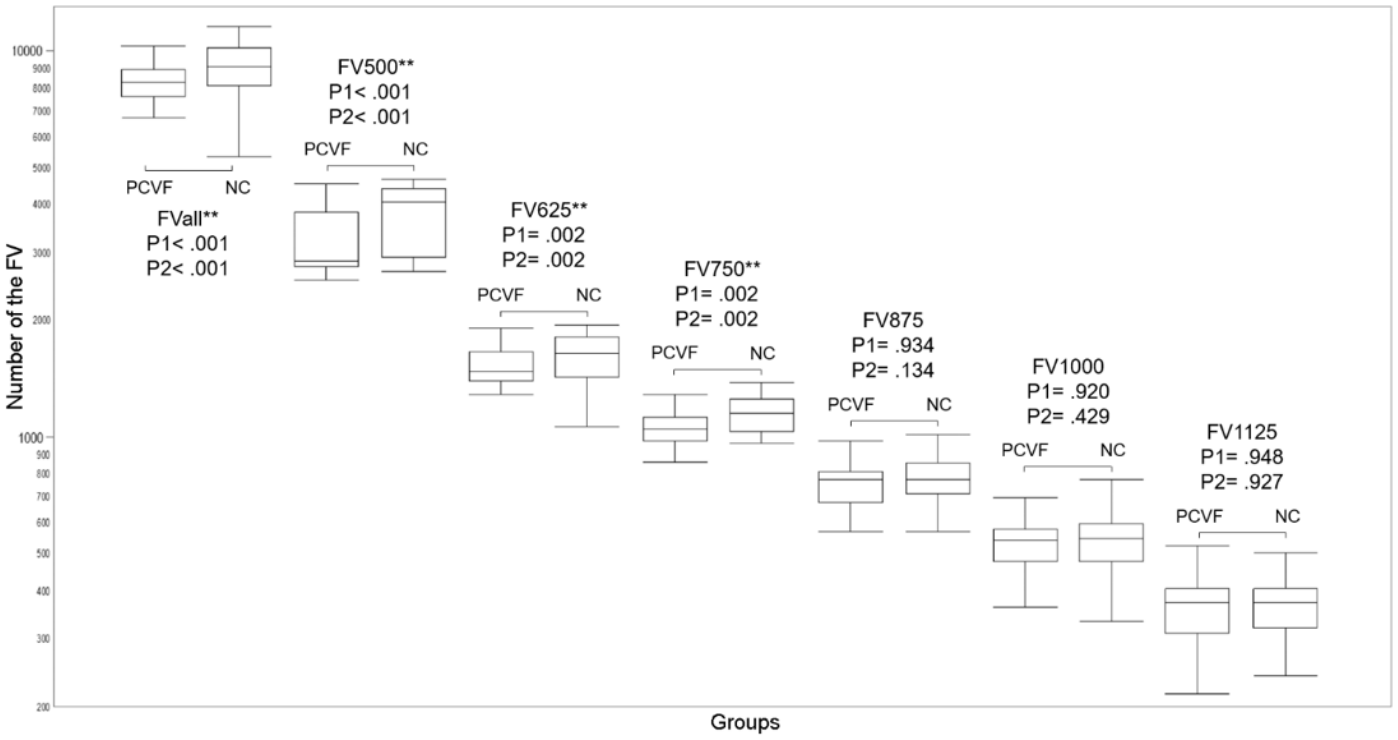

Figure 3

The comparison of flow void between the fellow eyes of PCV and normal controls. P1: The P-value of independent-samples median test. The number of FV were significantly lower in the PCVF compared to the controls in FVall, FV500, FV625, and FV750. And there were no differences among the two groups in FV875, FV1000, and FV1125. P2: The P-value of independent samples Mann-Whitney U test. The distribution was significantly different among the two groups, and the PCVF group had a higher central tendency in FVall, FV500, FV625, and FV750. And there were no differences among the two groups in FV875, FV1000, and FV1125. **P<.01 FV: The flow void of choriocapillaris. PCVF: The fellow eyes of PCV. controls: The age-matched normal control group. FVall: The FV sizes from 400μm2 to 25000μm2. FV500: The FV sizes from 400μm2 to 500μm2. FV625: The FV sizes from 525μm2 to 625μm2. FV750: The FV sizes from 650μm2 to 750μm2. FV875: The FV sizes from 775μm2 to 875μm2. FV1000: The FV sizes from 900μm2 to 1000μm2. FV1125: The FV sizes from 1025μm2 to 1125μm2.

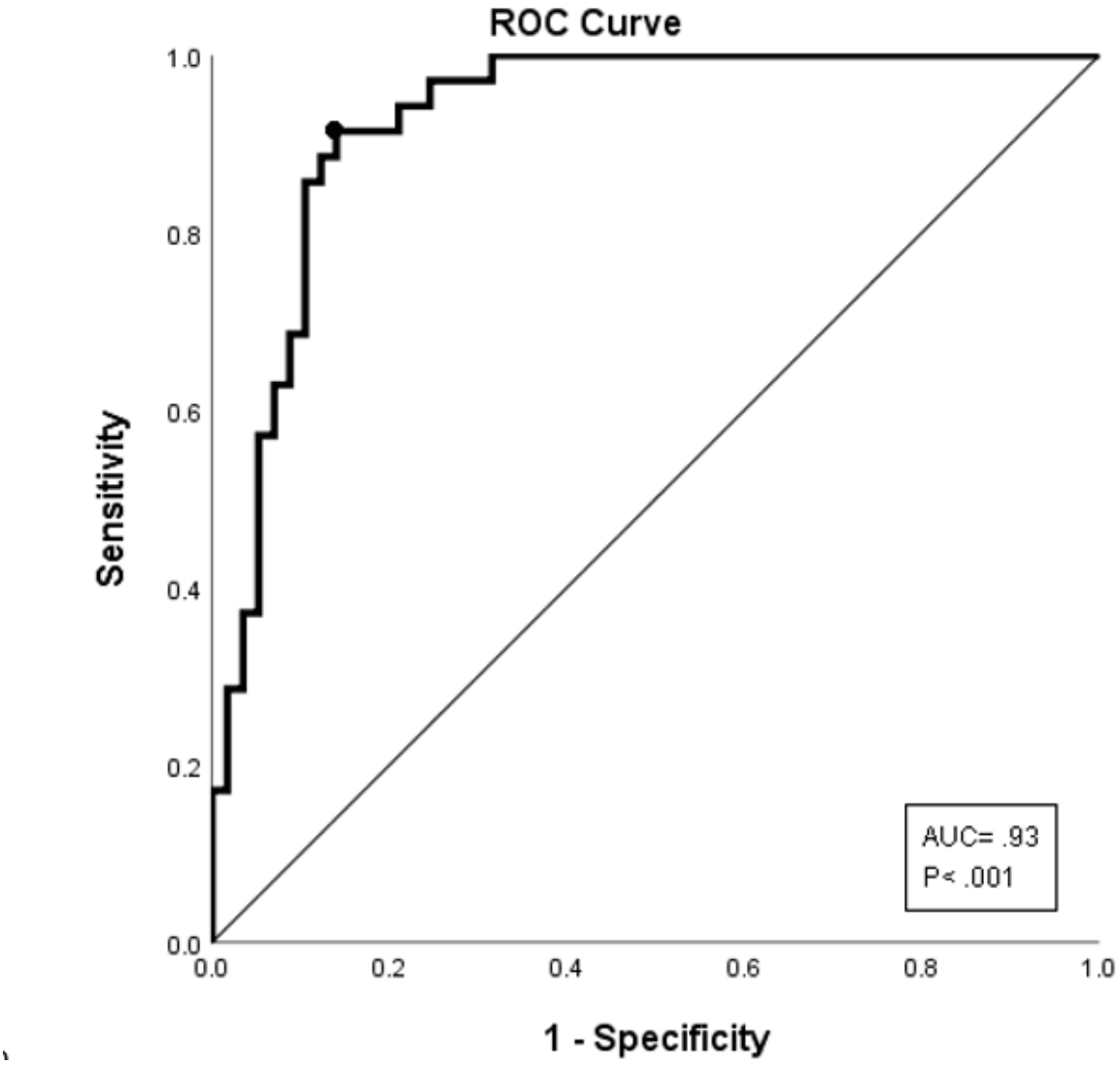

Figure 4

The receiver operating characteristic curve of the fellow eyes of PCV with choroidal vascular hyperpermeability and normal controls. The circled point is the best cut-off point. Youden index= .51, sensitivity= 91.4%, specificity = 86.0%. The area under the curve (AUC)= .93 (95% CI: .88~ .98) (P< .001).

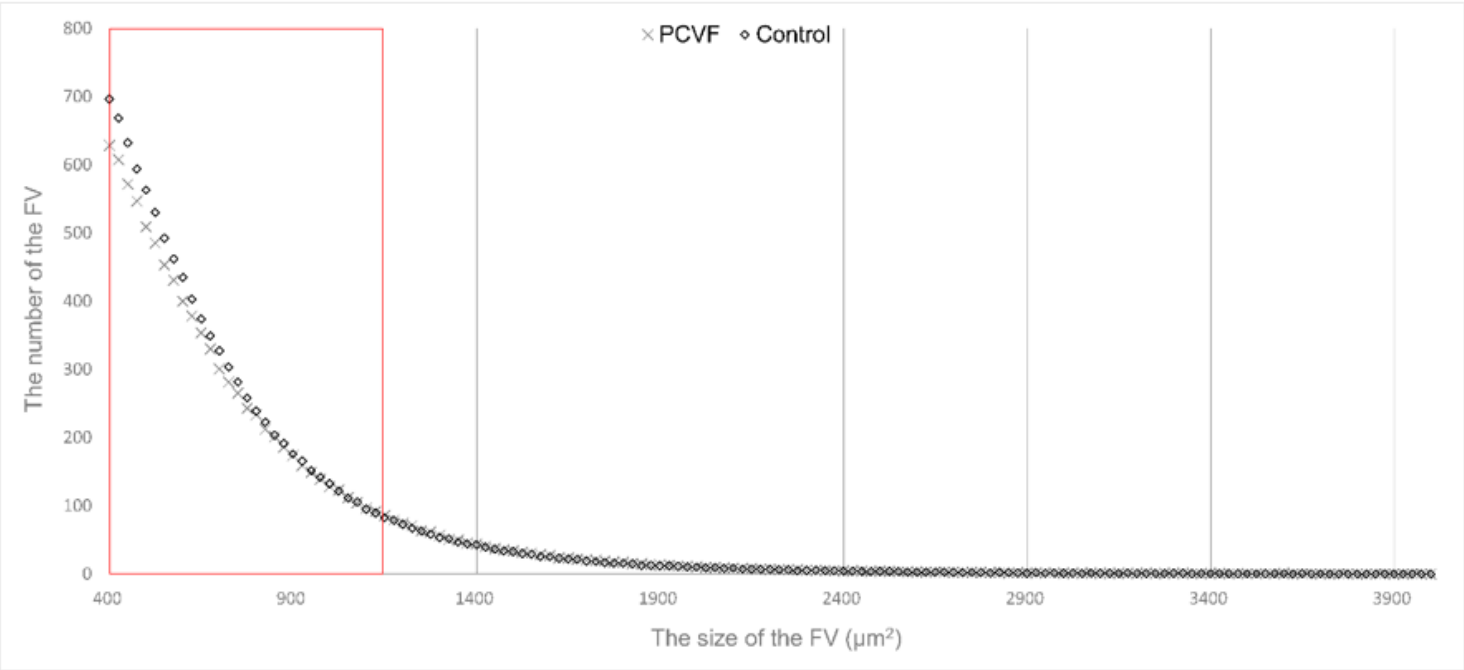

Figure 5

The demonstration of the FV distribution in a fellow eye of PCV with CVH and a control subject. The plot shows the typical power-law distribution of FV: The small sizes had relatively large numbers. The red box demonstrates our analysis strategy range. Our strategy focused on a specific range, which avoids the statistical biases due to the large disparity in numbers.